On the coupling of size-quantized excitons with light in one-dimensional dielectric-semiconductor photonic crystals

B. Flores-Desirena and R. Márquez-Islas
Facultad de Ciencias Físico Matemáticas, Benemérita Universidad Autónoma de Puebla, Apartado Postal 1152, Puebla, Pue. 72000, México.

N. Atenco-Analco
Escuela de Ciencias, Universidad Autónoma "Benito Juárez" de Oaxaca, Av. Universidad S/N, Ex-Hacienda de Cinco Señores, Ciudad Universitaria, Oaxaca de Juárez, Oax., 68120, México.

F. Pérez-Rodríguez
Instituto de Física, Benemérita Universidad Autónoma de Puebla, Apartado Postal J-48, Puebla, Pue. 72570, México, e-mail: fperez@sirio.ifuap.buap.mx

Recibido el 15 de julio de 2008; aceptado el 30 de agosto de 2008

The optical properties of exciton polaritons in one-dimensional photonic crystals are theoretically investigated. The periodic photonic structure is formed by two alternating layers, namely a local dielectric layer and a thin semiconductor one which is characterized by a nonlocal excitonic dielectric function. We calculate reflectivity spectra for one-dimensional MgO-CuCl photonic crystals, which exhibit a rich resonance structure because of the optical manifestation of size-quantized excitons. We study the changes in the resonance structure as the thickness of the thin semiconductor layer is varied. It is found that odd quantized-exciton modes are well manifest in the optical spectra in comparison with even states. We have also investigated the effect of both homogeneous bulk damping and interface-induced broadening upon the reflectivity resonances. The broadening due to interface disorder is calculated with the self-consistent Green's function method.

Keywords: Exciton; semiconductor nanostructures; photonic crystals.

Se estudian teóricamente las propiedades ópticas de polaritones excitónicos en cristales fotónicos con periodicidad unidimensional. La estructura periódica está formada por dos capas alternantes, a saber, una capa dieléctrica local y una capa semiconductora delgada que se caracteriza por una función dieléctrica no local. Calculamos espectros de reflectividad para un cristal unidimensional de MgO-CuCl el cual exhibe una estructura de resonancias debido a la manifestación óptica de excitones cuantizados en tamaño. Estudiamos los cambios en la estructura de resonancias conforme el espesor de la capa semiconductora delgada se varía. Se encontró que los modos impares de excitones cuantizados se manifiestan bien en los espectros ópticos en comparación con los estados pares. Hemos investigado también el efecto que tiene tanto el amortiguamiento de bulto homogéneo como el inhomogéneo inducido por las interfaces, sobre las resonancias de reflectividad. El ensanchamiento debido al desorden interfacial se calcula con el método autoconsistente de la función de Green.

Descriptores: Excitón; nanoestructuras semiconductoras; cristales fotónicos.

PACS: 71.35.-y; 78.20.-e; 78.66.-w; 78.67.-n; 78.67.De

1. Introduction

The quantization of excitons in different semiconductor heterostructures has been intensively investigated during the last three decades (see, for example, the reviews [1, 2]). There exist two regimes of exciton confinement: strong and weak confinement, which depend on the relation between the exciton Bohr radius a_B and the size l_s of the semiconductor medium. In the quantum well (strong confinement) regime $a_B \lesssim l_s$, whereas in the thin-film (weak confinement) regime $a_B \ll l_s$. In quantum wells, the motion of the electron and the hole are separately quantized [1,3–5], whereas in the thin-film regime their relative motion is the same as in the bulk except for a small distortion near film boundaries, which gives rise to exciton-free layers of thickness $l \sim a_B$. So, in the latter case, the center-of-mass motion of the exciton is quantized in an effective length $l_{eff} = l_s - 2l$ smaller than the real semiconductor film thickness l_s [1, 2, 6–8]. In both regimes, the exciton quantization is responsible for the appearance of resonances in the optical spectra. In the majority of the investigations the quantum-well or thin-film interfaces are assumed to be flat. However, realistic heterostructures have inherent roughness, which produces fluctuations in the exciton confining potential and, therefore, a substantial increase of both the inhomogeneous broadening ν_{inh} and the shift $\Delta\omega$ of exciton resonances [8–13]. So, in comparing theoretical spectra with experimental results, it is necessary to take into account ν_{inh} and $\Delta\omega$.

Among the large variety of heterostructures, the so-called photonic crystals (PC) are of great interest at present. The use of semiconductors as inclusions in such periodic structures can affect their spectral and optical properties near exciton resonance noticeably. As it is shown in the works [2,14–18], in the case of dielectric-semiconductor PCs

with weak exciton confinement, slightly-dispersive photonic bands appear at the eigenfrequencies of the size-quantized exciton states. Besides, the photonic band structure exhibits anticrossing phenomena as a result of the coupling of the photon-like mode with the size-quantized excitons. These changes in the photonic band structure lead to a complicated resonance structure of the optical spectra.

In this work we shall investigate the optical manifestation of size-quantized excitons in resonant dielectric-semiconductor photonic crystals with one-dimensional periodicity, *i.e.* in PCs composed of alternating dielectric and semiconductor thin films. In Sec.2, we shall calculate the reflectivity for the dielectric-semiconductor PC with the transfer-matrix method and a nonlocal model for the dielectric function of the semiconductor layers. Results for the reflectivity spectra of MgO-CuCl PCs will be presented and analyzed in Sec. 3. Here, we shall study the effect of the semiconductor-film thickness upon the resonance structure of the reflectivity. Besides, applying the method of the self-consistent Green's function, we shall calculate the inhomogeneous broadening ν_{inh} and shift $\Delta\omega$ of exciton resonances in thin films. The changes produced by the inherent interface roughness in the reflectance spectrum for PCs are also analyzed.

2. Theoretical formalism

2.1. Optical functions

Let us consider a one-dimensional photonic crystal formed by N unit cells. Each cell contains a dielectric layer (D) and a semiconductor one (S). The whole heterostructure contains an additional dielectric layer D as (DS)(DS)...(DS)D and overlies a local substrate. The axis z is assumed to be parallel to the growth direction, and the sample surface is at $z = -l_d$, where l_d is the thickness of the dielectric layers D. The interface between the heterostructure and the substrate is located at $z = N\Lambda$, where Λ is the width of the bilayer DS (see Fig. 1).

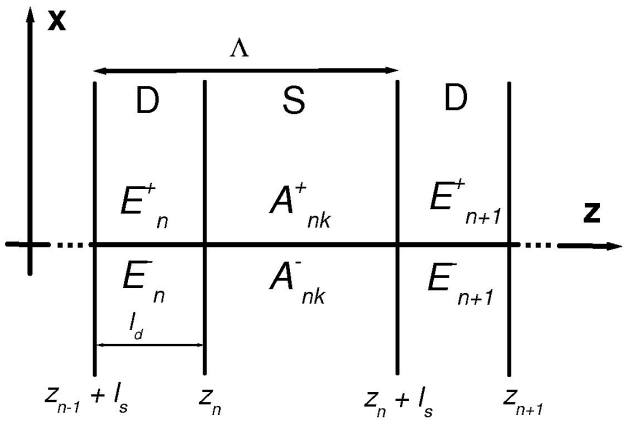

FIGURE 1. Scheme of the 1D dielectric-semiconductor photonic crystal.

Consider a monochromatic electromagnetic wave normally incident on the sample surface at $z = -l_d$. The electric field $\mathbf{E}_i$ of the incident electromagnetic wave is oriented along the y-axis. Thus, the electric field in the space $-\infty < z < -l_d$ can be written as

$$E_{ext}(z) = E_i e^{iq_i(z+l_d)} + E_r e^{-iq_i(z+l_d)}, \tag{1}$$

where E_i and E_r are the amplitudes of the incident and reflected electromagnetic waves, $q_i = \sqrt{\varepsilon_e}(\omega/c)$ is non-zero (z-) component of the wave vector, ε_e is the permittivity of the external medium, ω is the frequency, c is the light velocity for vacuum. In writing (1), we have omitted the factor $\exp(-i\omega t)$, describing the dependence of the electric field on time t.

The electric field inside the substrate is written in the form

$$E_{sub}(z) = E_t e^{iq_t(z-N\Lambda)} \ . \tag{2}$$

Here, $q_t = \sqrt{\varepsilon_s}(\omega/c)$ and ε_s is the permittivity of the substrate.

Inside the n-th local dielectric layer (Fig. 1), the electric field can be expressed as

$$E_{D,n}(z) = E_n^+ e^{iq_d(z-z_n+l_d)} + E_n^- e^{-iq_d(z-z_n)} \ ,$$
$$n = 1, 2, ..., N+1. \tag{3}$$

Here, $z_n = (n-1)\Lambda$, $q_d = \sqrt{\varepsilon_d}(\omega/c)$, and ε_d is the permittivity of the local dielectric layer.

Because of the normal incidence of light on the heterostructure, we can write the electric field in the n-th semiconductor layer (Fig. 1) as a combination of transverse bulk modes [19]:

$$E_{S,n}(z) = \sum_{k=1}^{2} \{A_{nk}^+ e^{iq_k(z-z_n)} + A_{nk}^- e^{-iq_k(z-z_n-l_s)}\}$$
$$n = 1, 2, ..., N. \tag{4}$$

Here, $l_s = \Lambda - l_d$ is the thickness of the semiconductor layer, q_1, q_2 denote the wave vectors of the transverse bulk exciton-polaritons and are given by the solution of the equation

$$q_z^2 = \frac{\omega^2}{c^2}\varepsilon(q_z, \omega) \ ,$$
$$\varepsilon(q_z, \omega) = \varepsilon_\infty + 4\pi\chi(q_z, \omega) \ , \tag{5}$$

ε_∞ is the high-frequency dielectric constant, and $\chi(q_z, \omega)$ is the excitonic contribution to the dielectric susceptibility, which is given by

$$\chi(q_z, \omega) = \frac{\omega_s^2/4\pi}{\omega_T^2 - \omega^2 + Dq_z^2 - i\omega\gamma_s} \ . \tag{6}$$

Here, ω_T stands for the transverse resonance frequency, ω_s is a measure of the oscillator strength, γ_s is the exciton relaxation frequency, and $D = \hbar\omega_T/M$ is the parameter describing the spatial dispersion (M denotes the total mass of

the exciton). The Eq. (5) for the wave vector q_z has four solutions, namely

$$q_{1,2} = \left\{ \frac{1}{2} \left[\Gamma_B^2 + \varepsilon_\infty \frac{\omega^2}{c^2} \pm \left(\left[\Gamma_B^2 - \varepsilon_\infty \frac{\omega^2}{c^2} \right]^2 + \frac{4\omega_s^2 \omega^2 M}{\hbar \omega_T c^2} \right)^{1/2} \right] \right\}^{1/2} , \quad (7)$$

$$q_{3,4} = -\, q_{1,2}, \quad (8)$$

where q_1 and q_2 are the square roots with positive imaginary part ($\Im q_1 > 0$, $\Im q_2 > 0$), and Γ_B^2 is defined as

$$\Gamma_B^2 = \frac{1}{D} \left[\omega^2 - \omega_T^2 + i\omega\gamma_s \right] . \quad (9)$$

Acoording to Eqs. (4)-(6), the response of the semiconductor layers is assumed to be bulk-like. Hence, the excitonic polarization P_n in the semiconductor layer of the n-th cell can be written as

$$P_n(z) = \sum_{k=1}^{2} \chi(q_k, \omega) \times \{ A_{nk}^{+} e^{iq_k(z-z_n)} + A_{nk}^{-} e^{-iq_k(z-z_n-l_s)} \}. \quad (10)$$

In order to calculate optical functions, we should determine the amplitudes of the electromagnetic fields inside all the layers by applying Maxwell boundary conditions: the continuity of the tangential components of the electric and magnetic field at all the interfaces $z = z_n$ and $z = z_n + l_s$. These conditions can be written as follows

$$E_{D,n}(z_n) = E_{S,n}(z_n) ,$$
$$E_{D,n}^{'}(z_n) = E_{S,n}^{'}(z_n) , \quad (11)$$
$$E_{S,n}(z_n + l_s) = E_{D,n+1}(z_n + l_s) ,$$
$$E_{S,n}^{'}(z_n + l_s) = E_{D,n+1}^{'}(z_n + l_s) . \quad (12)$$

The continuity of the derivatives of the electric field in (11) and (12) follows directly from the Faraday law, $B(z) = (ic/\omega)E^{'}(z)$, in a nonmagnetic medium ($\mathbf{H} = \mathbf{B}$).

The Eq. (12) are not enough for determining the amplitude of the additional electromagnetic waves that are generated in the nonlocal semiconductor. Therefore, we should apply additional boundary conditions (ABC). In the case of semiconductors characterized by excitons with very small Bohr radius [19–21], it is appropriate to apply the Pekar ABC [22]: The vanishing of the excitonic polarization at the boundaries of the semiconductor, *i.e.*,

$$P_n(z_n) = 0 , \qquad P_n(z_n + l_s) = 0 . \quad (13)$$

Employing the expressions (3), (4) and (10) for the polaritonic fields and the boundary conditions (11), (12) and (13), we obtain a relation between the amplitudes E_{n+1}^{+}, E_{n+1}^{-} and the amplitudes E_n^{+}, E_n^{-}:

$$\begin{pmatrix} E_{n+1}^{+} \\ E_{n+1}^{-} \end{pmatrix} = \mathcal{M} \begin{pmatrix} E_n^{+} \\ E_n^{-} \end{pmatrix} , \quad (14)$$

where $\mathcal{M}$ is the transfer matrix, which is straightforwardly calculated [2]. In determining the optical properties, we also use the boundary conditions at the sample surface ($z = -l_d$), and at the interface between the dielectric-semiconductor heterostructure and the substrate ($z = N\Lambda$):

$$E_{ext}(-l_d) = E_{D,1}(-l_d) ,$$
$$E_{ext}^{'}(-l_d) = E_{D,1}^{'}(-l_d) , \quad (15)$$
$$E_{D,N+1}(N\Lambda) = E_{sub}(N\Lambda) ,$$
$$E_{D,N+1}^{'}(N\Lambda) = E_{sub}^{'}(N\Lambda). \quad (16)$$

The relationship between the amplitudes of the electric field in the first and last local dielectric (D) layers is established by using (14) iteratively. Afterwards, the reflectivity R, transmission T and absorption A are calculated from Eqs. (15) and (16):

$$R = \left| \frac{E_r}{E_i} \right|^2 , \quad T = \frac{q_t}{q_i} \left| \frac{E_t}{E_i} \right|^2 , \quad A = 1 - R - T. \quad (17)$$

2.2. Inhomogeneous broadening

The behavior of excitons in semiconductor thin-film heterostructures is generally studied by assuming that the thin-film interfaces are flat. However, the inherent surface roughness yield fluctuations in the exciton center-of-mass confining potential and, consequently, a considerable increase in the inhomogeneous broadening ν_{inh} as well as a shift $\Delta\omega$ of exciton resonances. Both quantities, ν_{inh} and $\Delta\omega$, depend on the frequency and, hence, can modify optical spectra [23,24]. In the majority of works [20, 25–29], where the effect of the exciton scattering by the disordered interfaces on the optical response of thin films has been considered, models without strict derivation were employed. A Green's function formalism to calculate the inhomogeneous broadening and shift of exciton resonances in the thin film regime was proposed in Ref. 12. In this subsection, we shall revise such a formalism and apply it to one-dimensional photonic crystals with semiconductor thin films. In other words, we shall calculate the contribution of the interface disorder to the relaxation frequency γ_s appearing in the resonant exciton susceptibility Eq. (6) of each semiconductor thin layer.

Consider an excitonic film occupying the space $\xi(x) \leq z \leq l_s$, where $\xi(x)$ is a random function, representing the surface profile of the film. For simplicity and without loss of generality, the surface roughness is assumed to be one-dimensional. We also suppose that the roughness is a stationary random process characterized by the properties:

$$\langle \xi(x) \rangle = 0 , \qquad \langle \xi(x)\xi(x') \rangle = \zeta^2 W(|x - x'|) , \quad (18)$$

where the angular brackets denote statistical average over the ensemble of realizations of the function $\xi(x)$, ζ is the root mean square of the roughness height and $W(|x|)$ is the correlation function which has a typical scale R_c of monotonous decrease (R_c is the correlation radius). Thus, one of the thin-film surfaces is randomly rough, whereas the other one is, for simplicity, flat. Such a system is physically equivalent to a film with both surfaces being rough, statistically identical, and not intercorrelated [30]. We shall also assume that R_c is much larger than the r.m.s. height ζ and the exciton Bohr radius a_B ($R_c \gg \zeta$, $R_c \gg a_B$), *i.e.* the rough surface is rather smooth. Besides, we shall consider the case when the wavelength of the incident light is much larger than ζ ($q_i\zeta \ll 1$).

The Hamiltonian for the translational motion of the $1s$ exciton can be expressed as

$$\hat{H} = -\frac{\hbar^2}{2M}\nabla^2 + E_g + E_1^r\,, \tag{19}$$

where, E_1^r is the ground-state eigenenergy for the relative motion, $M = m_e + m_h$ is the total exciton mass, m_e and m_h are, respectively, the effective electron and hole masses, and E_g is the energy gap between valence and conduction bands. The spectrum for the exciton in a surface-disordered film can be calculated from the retarded Green's function $G(\mathbf{r}, \mathbf{r}')$, which satisfies the equation

$$[E + i\hbar\nu_0 - \hat{H}]G(\mathbf{r}, \mathbf{r}') = \delta(\mathbf{r} - \mathbf{r}')\,. \tag{20}$$

with "no escape" boundary conditions:

$$G(z = \xi(x)) = 0\,, \qquad G(z = l_s) = 0\,. \tag{21}$$

In Eq. (20), E stands for the total exciton energy, $\hbar\nu_0$ is the homogeneous bulk damping, and $\mathbf{r} = (x, z)$ is a two-dimensional vector, indicating the exciton center-of-mass coordinates. For the case of a rough surface, which is sufficiently smooth, we can expand Eq. (21) up to first order in $\xi(x)$. We get an approximate boundary condition:

$$G(z = 0) + \xi(x)\,\frac{\partial G}{\partial z}\bigg|_{z=0} = 0, \tag{22}$$

Now, applying the Green's theorem, we can establish a relationship between the Green's function G, perturbed by the surface disorder, and the Green's function G_0 for the ideal thin film with $\xi(x) = 0$. This relationship has the form of a Dyson-type integral equation:

$$G(\mathbf{r}, \mathbf{r}') = G_0(\mathbf{r}, \mathbf{r}') + \int_{-\infty}^{\infty} dx_1 G_0(\mathbf{r}, \mathbf{r}_1) V(\mathbf{r}_1) G(\mathbf{r_1}, \mathbf{r}')\,, \tag{23}$$

where the kernel $V(\mathbf{r}_1)$ is the exciton center-of-mass scattering potential and, in the linear approximation in ξ, has the form

$$V(\mathbf{r}_1) \equiv \frac{\overleftarrow{\partial}}{\partial z_1}\bigg|_{z_1=0} \frac{\hbar^2}{2M}\,\xi(x_1)\,\frac{\vec{\partial}}{\partial z_1}\bigg|_{z_1=0}\,. \tag{24}$$

Here, the arrows over the derivatives denote the direction of the operation, *i.e.* $\leftarrow$ ($\rightarrow$) means derivation of a function written on the left (right) of $V(\mathbf{r}_1)$.

In order to calculate the exciton spectrum in the surface-disordered thin film, we should average Eq. (23) for the Green's function G. After applying the technique proposed in [31], we get an equation for the average Green's function $\langle G\rangle$ within the self-consistent Born approximation [12, 32], which can be written as

$$\langle G\rangle = G_0 + G_0\langle\,\hat{V}\,\langle G\rangle\,\hat{V}\,\rangle\langle G\rangle\,, \tag{25}$$

where $\hat{V}(\mathbf{r_1})$ is an integral operator of the random scattering potential $V(\mathbf{r_1})$. The solution of Eq. (25) within the polar approximation [32] is given by

$$\langle G(x - x'; z, z')\rangle = \int_{-\infty}^{\infty} \frac{dk_x}{2\pi}\,\langle \mathcal{G}(k_x; z, z')\rangle \times \exp[ik_x(x - x')]\,, \tag{26}$$

where

$$\langle \mathcal{G}(k_x; z, z')\rangle = \frac{\mathcal{G}_0(k_x; z, z')}{1 - \,k_z\cot(k_z l_s)\,\mathcal{K}(k_x)}\,. \tag{27}$$

Here, k_z is the transverse component of the wave vector $\mathbf{k}$ and is defined by the expression:

$$k_z(k_x) = \left[\frac{2M}{\hbar^2}\,[\hbar\omega - \hbar\omega_T + i\hbar\nu_0] - k_x^2\right]^{1/2}\,, \tag{28}$$

where $\hbar\omega = E$, and $\omega_T = (E_g + E_1^r)/\hbar$ is the $1s$ exciton resonance frequency. Due to the self-consistency of our approach, the quantity $\mathcal{K}$ should be calculated from an integral equation that follows straightforwardly from Eq. (25). Such an equation has the form

$$\mathcal{K}(k_x) = \int_{-\infty}^{\infty} \frac{dk_x'}{2\pi}\,\mathcal{W}(k_x - k_x')\,\triangle_{\mathcal{K}}(k_x')\,k_z'\,, \tag{29}$$

where

$$\triangle_{\mathcal{K}}(k_x') = \frac{\zeta^2\,\cot(k_z' l_s)}{1 - \,k_z'\cot(k_z' l_s)\,\mathcal{K}(k_x')}\,, \tag{30}$$

and $\mathcal{W}(k_x)$ is the Fourier transform of the correlator $W(|x|)$ (18).

In the case of an ideal thin film ($\xi = 0$),

$$\langle \mathcal{G}(k_x; z, z')\rangle = \mathcal{G}_0(k_x; z, z')$$

and, hence, exciton resonances appear at frequencies satisfying the relation $k_z(\omega_n)l_s = n\pi$ ($n = 1, 2, ...$). However, as it follows from Eq. (27), such resonances will be broadened and shifted by the exciton center-of-mass scattering from the thin-film rough surface. In order to determine

the inhomogeneous broadening ν_{inh}, as well as the shift $\Delta\omega$ of the exciton resonances, we should find the poles of the function $\langle \mathcal{G}(k_x; z, z')\rangle$, *i.e.* we have to solve the equation

$$\tan(k_z l_s) = k_z \mathcal{K}(k_x)\,. \tag{31}$$

At values $k_z l_s \approx n\pi$, Eq. (31) can be rewritten as

$$k_z^2 - \frac{2}{l_s}\, k_z^2 \mathcal{K}(k_x) - \left(\frac{n\pi}{l_s}\right)^2 = 0\,. \tag{32}$$

Using (28), the equation for the poles of the function $\langle \mathcal{G}(k_x; z, z')\rangle$ acquires the form

$$\hbar\omega - \hbar\omega_T - \frac{\hbar^2}{2M}\left(\frac{n\pi}{l_s}\right)^2 - \frac{\hbar^2 k_x^2}{2M} + i\hbar\nu_0 - \frac{\hbar^2}{M l_s}\, k_z^2 \mathcal{K}(k_x) = 0\,. \tag{33}$$

Hence, the imaginary and real parts of the last term in the left-hand side of Eq. (33) determine the inhomogeneous broadening ν_{inh} and the shift $\Delta\omega$ of exciton resonances:

$$\nu_{inh}(\omega) = -\,\frac{\hbar}{M l_s}\, \Im[k_z^2\, \mathcal{K}(k_x)]\,, \tag{34}$$

$$\triangle\omega(\omega) = \frac{\hbar}{M l_s}\, \Re[k_z^2\, \mathcal{K}(k_x)]\,. \tag{35}$$

According to the formulas (34) and (35), the surface-induced broadening $\nu_{inh}(\omega)$ and shift $\Delta\omega(\omega)$ of exciton resonances depend on the statistical parameters of the surface disorder, the exciton characteristics and the average thickness of the film l_s. So, the effect of surface roughness becomes more important as the thickness l_s decreases. Besides, the frequency dependence of ν_{inh} and $\Delta\omega$ is determined by the ratio of the variation scales $1/R_c$ and $\sqrt{2M(\nu_0+\nu_{inh})/\hbar}$ of the functions $\mathcal{W}(k_x)$ (29) and $\triangle_{\mathcal{K}}(k_x)$ (30), respectively.

In calculating optical functions, we shall neglect the relatively small energy associated with light scattered in directions different from those of reflection and transmission [33] because $q_i\zeta \ll 1$. Within this approximation the average reflectivity R and transmissivity T can be calculated from boundary conditions for the exciton-polariton fields, satisfying Maxwell equations with the ensemble-averaged excitonic polarization

$$P(x, z, \omega) = -2|M|^2 \int dx' \times \int dz' \langle G(|x - x'|; z, z')\rangle E(x', z', \omega), \tag{36}$$

where M is a measure of the interband transition dipole density, and the average Green function $\langle G(|x - x'|; z, z')\rangle$ is given by Eqs. (26) and (27). Hence, for normal incidence of light the formulae (34) and (35) should be evaluated at $k_x = 0$ [8–13]. Nevertheless, these formulae can also be used within the framework of the formalism developed in previous section for calculating optical spectra. Indeed, since the frequency dependence of the inhomogeneous broadening $\nu_{inh}(\omega)$ and shift $\Delta\omega(\omega)$ is quantitatively correct in the neighborhood of the size-quantized exciton resonances and exciton effects on optical spectra are negligible far from resonances, we can use them as a frequency-dependent constant damping and a resonance shift in the exciton susceptibility. So, comparing the left-hand side of Eq. (33) with the denominator of the resonant exciton susceptibility (6), it follows that the inhomogeneous broadening ν_{inh} is related with the constant damping γ_s as

$$\gamma_s = 2(\nu_0 + \nu_{inh}), \tag{37}$$

and, moreover, the exciton resonance is shifted by the quantity

$$\Delta\omega_T = 2\Delta\omega. \tag{38}$$

3. Results

3.1. Effect of semiconductor-layer thickness

The theory developed in the previous section is valid for semiconductors with very small exciton Bohr radius a_B. An example of such a kind of semiconductor is CuCl, which possesses a large binding energy (~ 190 meV) and a Bohr radius $a_B \sim 7\mathring{A}$. Therefore, the thin-film regime can be observed up to a rather small thickness, l_s, of the order of a few nanometers. As it is known [19–21, 25, 26], the presence of ultra-narrow exciton-free layers in CuCl thin-film heterostructures can be neglected in interpreting their optical spectra.

Now, let us calculate the reflectivity of 1D dielectric-semiconductor PCs, having a unit cell with CuCl (S layer) and MgO (D layer) inclusions. The CuCl parameters used are [17]: the exciton mass $M = 2.5m_0$ (m_0 is the free electron mass), $\hbar\omega_T = 3.2022$eV, $\hbar\omega_L = 3.2079$eV for the transverse and longitudinal exciton frequencies, respectively, and a high frequency permittivity $\varepsilon_\infty = 5.0$. The permittivity for MgO used is $\varepsilon_d = 3.1$. The thickness of the semiconductor layer for each sample is, correspondingly, $l_s = 105\mathring{A}$ (Fig. 2), $130\mathring{A}$ (Fig. 3), $165\mathring{A}$ (Fig. 4) and the lattice constant is $\Lambda = 813\mathring{A}$. In the calculation we have considered $N = 200$ unit cells and a very small damping $\gamma_s = 0.001$meV. The medium outside the dielectric-semiconductor PC is assumed to be vacuum.

The panels (c) in Figs. 2, 3 and 4 exhibit the reflectivity spectra for the dielectric-semiconductor PCs near the exciton resonance frequency. In order to interpret them, we show the dispersion curves (panels "a") for the transverse bulk exciton-polariton modes, which are calculated from Eq. (7), and the bulk photonic dispersion for the PC in the narrow frequency range of the exciton resonance (panels "b"). The latter bulk dispersion is obtained by the standard way [2]. That is, we model the real finite heterostructure with a large number of cells ($N \gg 1$) as an infinite periodic one.

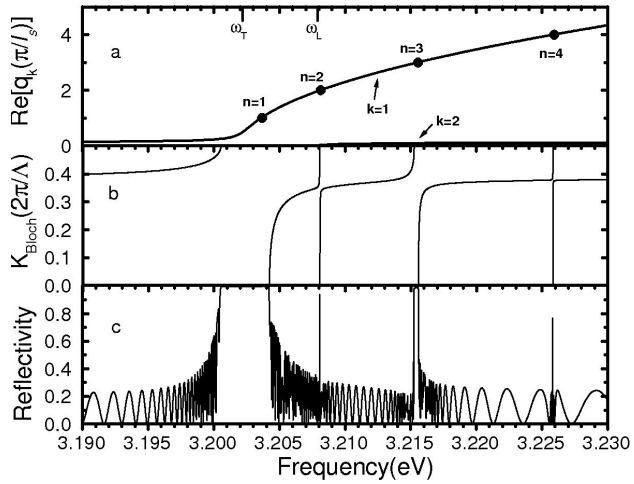

FIGURE 2. a) Dispersion curves for the transverse exciton-polariton modes in CuCl. The curve labeled with $k = 1$ ($k = 2$) corresponds to the exciton-like (photon-like) mode. Polariton dispersion (b) and reflectivity spectrum (c) for a MgO-CuCl 1D photonic crystal, which were calculated with a CuCl-layer thickness $l_s = 105\mathring{A}$ and a lattice constant $\Lambda = 813\mathring{A}$. The points in panel (a) indicate the eigenfrequencies of the quantized excitons with $q_1 l_s = n\pi$, $n = 1, 2, ...$

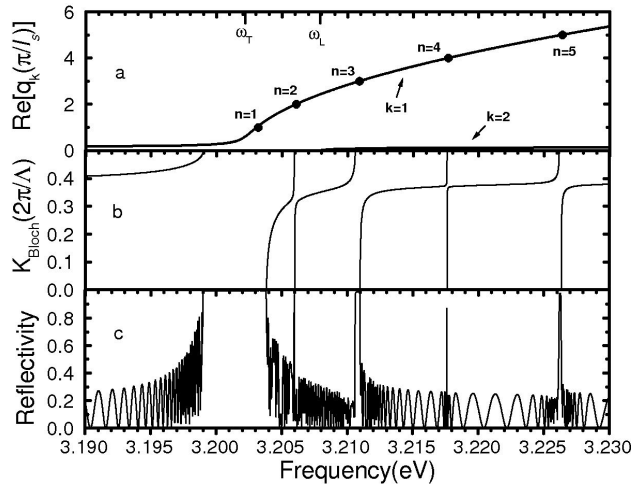

FIGURE 3. a) Dispersion curves for the transverse exciton-polariton modes in CuCl. Polariton dispersion (b) and reflectivity spectrum (c) for a MgO-CuCl 1D photonic crystal, which were calculated with a CuCl-layer thickness $l_s = 130\mathring{A}$ and a lattice constant $\Lambda = 813\mathring{A}$.

Then, we apply the Bloch theorem for the electric field in the PC,

$$E(z,t) = E_{K_B}(z) e^{iK_B z} e^{-i\omega t} , \tag{39}$$

where K_B is the Bloch wave vector and $E_{K_B}(z)$ is a periodic function with the same period as for the PC:

$$E_{K_B}(z) = E_{K_B}(z + \Lambda) . \tag{40}$$

Using the expression (39), we get a relation for the electric fields (3) in the local (D) layers:

$$\begin{pmatrix} E_n^+ \\ E_n^- \end{pmatrix} = e^{-iK_B\Lambda} \begin{pmatrix} E_{n+1}^+ \\ E_{n+1}^- \end{pmatrix} . \tag{41}$$

Substituting (14) into (41), the later equation can be rewritten in the form

$$\mathcal{M} \begin{pmatrix} E_n^+ \\ E_n^- \end{pmatrix} = e^{iK_B\Lambda} \begin{pmatrix} E_n^+ \\ E_n^- \end{pmatrix} . \tag{42}$$

The dispersion law for the bulk electromagnetic modes in the PC is obtained by requiring that the determinant of the matrix for the homogeneous algebraic system of equations (42) be equal to zero:

$$\left| \mathcal{M} - \mathcal{I} e^{iK_B\Lambda} \right| = 0 , \tag{43}$$

where $\mathcal{I}$ is the unit matrix. In the calculation of bulk exciton-polariton (panels "a") and photonic (panels "b") dispersion curves the exciton damping was neglected ($\gamma_s = 0$). As it was shown in Ref. [17], because of exciton-photon coupling in the photonic crystal, the bulk exciton-polariton dispersion splits into bands separated by small gaps (compare panels "a" with "b"). These bands are slightly dispersive and their energy values coincide with the eigenfrequencies of the size-quantized exciton:

$$\omega_n = \omega_T + \frac{\hbar}{2M} \left(\frac{n\pi}{l_s} \right)^2 , \tag{44}$$

where $n = 1, 2, ...$ Also, there is anticrossing of such bands and the upper (photon-like) branch of the bulk exciton-polariton ($k = 2$ in panels "a"). As is seen in Figs. 2 to 4, the reflectivity is close to one in the gap near the exciton resonance frequency ω_T and has sharp resonances at the frequencies $\omega = \omega_n$ corresponding to the size-quantized exciton states Eq. (44). It is interesting that the so-called polariton effect (a small shift of the resonances with respect to the eigenvalues ω_n due to the exciton-photon coupling)

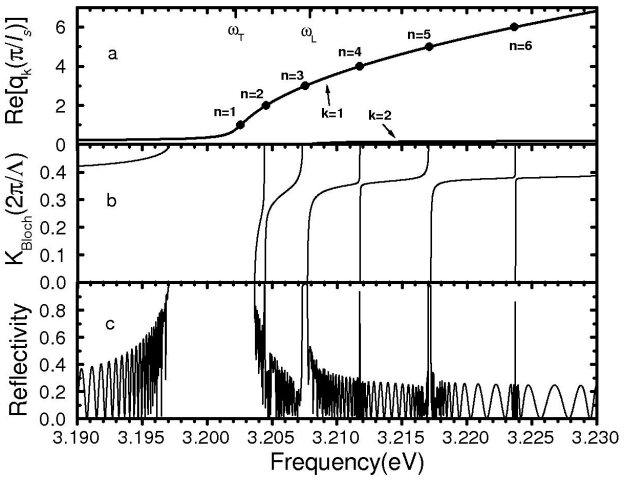

FIGURE 4. a) Dispersion curves for the transverse exciton-polariton modes in CuCl. Polariton dispersion (b) and reflectivity spectrum (c) for a MgO-CuCl 1D photonic crystal, which were calculated with a CuCl-layer thickness $l_s = 165\mathring{A}$ and a lattice constant $\Lambda = 813\mathring{A}$.

is practically absent for the samples considered here, unlike heterostructures containing thicker CuCl films [19–21]. In addition, because of the small thickness l_s of the CuCl layers, the frequency interval between consecutive quantized-exciton states ($\hbar\pi^2/(2Ml_s^2)$) turns out to be of the same order as the longitudinal transverse splitting $\omega_{LT} \equiv \omega_L - \omega_T$ (see Figs. 2 to 4). Note that the width of the lowest frequency gap decreases as the thickness l_s of the semiconductor layer is reduced (compare panels "c" of Figs. 2 to 4.)

From the inspection of Figs. 2 to 4, it is also evident that the resonances corresponding to odd quantized-exciton states ($n = 1, 3, ...$) are clearly manifest, whereas the even modes ($n = 2, 4, ...$) produce very weak resonances. This result agrees with the prediction for single films, having a thickness l_s much smaller than the photon wavelength ($\omega l_s/2\pi c \ll 1$) [25, 26].

3.2. Effect of damping

Now, let us analyze the effect of both homogeneous bulk broadening and the interface disorder on reflectivity spectra for one-dimensional CuCl-MgO PCs considered in the previous subsection. Using the formalism developed in Sec. 2.2, we have calculated the surface-induced broadening ν_{inh} and shift $\Delta\omega$ (see Fig. 5) in the Z_3 exciton region of a CuCl thin film. In the calculation we have taken into account the geometry of normal incidence of light ($k_x = 0$) and a Gaussian correlation function. The CuCl parameters used are indicated in the previous subsection. We also use a thin film thickness $l_s = 165\,\mathring{A}$, a r.m.s. height $\zeta = 12\,\mathring{A}$, a correlation radius $R_c = 100\,\mathring{A}$, and a homogeneous bulk broadening $\nu_0 = 0.3$ meV. As it is seen in Fig. 5a, the inhomogeneous broadening ν_{inh} exhibits relatively wide resonances at frequencies close to the eigenvalues of the size-quantized exciton in an ideal thin film: $\omega_n = \omega_T + (\hbar/2M)(n\pi/l_s)^2$. Moreover, at frequencies $\omega > \omega_T$, the average value of $\nu_{inh}(\omega)$ increases considerably.

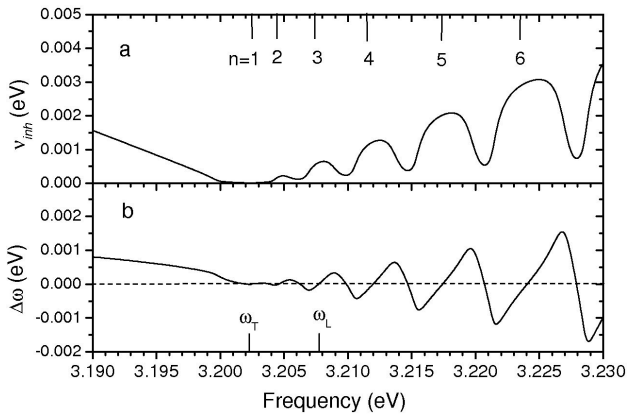

FIGURE 5. Inhomogeneous broadening ν_{inh} and shift $\Delta\omega$ of Z_3 exciton resonance in a CuCl thin film.

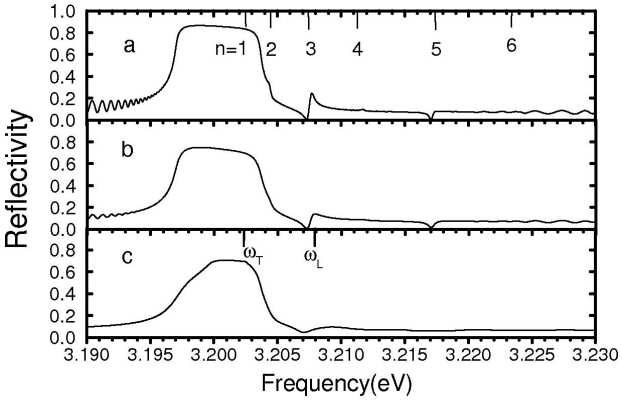

FIGURE 6. Reflectivity spectra for a MgO-CuCl 1D photonic crystal as in Fig. 4, with $\gamma_s = 0.3$ meV (a), 0.6 meV(b), and $\gamma_s = 2(\nu_0 + \nu_{inh})$ (c), where $\nu_0 = 0.3$ meV and ν_{inh} is taken from Fig. 5a.

This behavior agree with previous phenomenological models [20, 27, 28] used to explain optical spectra of CuCl thin films. The exciton resonance shift $\Delta\omega$ undergoes oscillations as a function of frequency ω (see Fig. 5b).Unlike inhomogeneous broadening, the shift $\Delta\omega$ vanishes at frequencies close to the eigenvalues ω_n of the size-quantized exciton. For calculating the reflectivity spectrum of a one-dimensional dielectric-semiconductor PC with interface disorder, we shall assume that the PC is composed of thin films, whose rough interfaces are statistically equivalent. Under these conditions, the damping constant γ_s (37) is assumed to be the same for all the thin films. On the other hand, considering that the shift $\Delta\omega$ vanishes near exciton resonances, we shall neglect it in calculating the reflectivity of MgO-CuCl PC . In Fig. 6, we present the reflectivity spectra calculated for the same PC as in Fig. 4, but with

a) $\gamma_s = 0.3$ meV ($\nu_0 = 0.15$ meV, $\nu_{inh} = 0$),

b) $\gamma_s = 0.6$ meV ($\nu_0 = 0.3$ meV, $\nu_{inh} = 0$), and

c) $\gamma_s = 2(\nu_0 + \nu_{inh})$ ($\nu_0 = 0.3$ meV),

and ν_{inh} taken from Fig. 5a. Comparing the reflectivity spectra in Figs. 4 and 6, it is seen that both Fabry-Perot resonances, due to the finite size ($N\Lambda + l_d$) of the whole heterostructure, and those associated with the size-quantized excitons in thin semiconductor layers are smoothed out as both the homogeneous bulk broadening ν_0 (panels (a) and (b)) in Fig. 6 and the surface-induced damping ν_{inh} (panel (c)) are increased. So, the manifestation of size-quantized excitons in optical spectra of one-dimensional PC depends strongly on the quality of its interfaces. It is interesting, however, that the width of the lowest gap in the photonic dispersion, which results from the anticrossing between the photonic and excitonic modes, turns out to be slightly affected by damping.

4. Conclusion

We have investigated the spectral and optical properties of one-dimensional dielectric-semiconductor photonic crystals.

In particular, we have studied the quantization of the exciton center-of-mass motion in very thin films and its manifestation in reflectivity spectra for PCs. The calculation of the reflectivity is based on the use of a nonlocal dielectric function for the semiconductor film. It was found that the decrease of the thickness of the semiconductor films reduces the width of the lowest frequency gap in the photonic dispersion. We have also considered PCs with interface disorder. In this case, the inhomogeneous broadening of exciton resonances is considerable and should be taken into account in calculating optical spectra. The formalism of the self-consistent Green's function was revised and applied to derive explicit expressions for the inhomogeneous broadening and shift of exciton resonances. Finally, we have compared the reflectivity spectra for PCs with and without interface disorder.

Acknowledgments

This work was partially supported by CONACYT (grant SEP-2004-C01-46425) and VIEP-BUAP (Grants 35/EXC-08/I and 96/EXC-09/G).

1. L.C. Andreani, in *Confined Electrons and Photons: New Physics and Devices*, edited by E. Burstein and C. Weisbuch (Plenum Press, New York, 1994).
2. G.H. Cocoletzi and W.L. Mochán, *Surf. Sci. Rep.* **57** (2005) 1.
3. F. Tassone, F. Bassani, and L.C. Andreani, *Phys. Rev. B* **45** (1992) 6023.
4. R. Atanasov, F. Bassani, and V.M. Agranovich, *Phys. Rev. B* **49** (1994) 2658.
5. N. Atenco-Analco, B. Flores-Desirena, A. Silva-Castillo, and F. Pérez-Rodríguez, *Superficies y Vacío* **13** (2001) 134.
6. F. Bassani, M. Dressler, and G. Czajkowski, *Il Nuovo Cimento D* **20** (1998) 1355.
7. H. C. Schneider, F. Jahnke, S. W. Koch, J. Tignon, T. Hasche, and D. S. Chemla, *Phys. Rev. B* **63** (2001) 045202.
8. N. Atenco-Analco, N. M. Makarov, and F. Pérez-Rodríguez, *Solid State Commun.* **119** (2001) 163.
9. N. Atenco-Analco, N.M. Makarov, and F. Pérez-Rodríguez, *Microel. J.* **33** (2002) 375.
10. N. Atenco-Analco, N.M. Makarov, and F. Pérez-Rodríguez, *Phys. Stat. Sol. (c)* **0** (2003) 2921.
11. N. Atenco-Analco, N. M. Makarov, F. Pérez-Rodríguez, *Rev. Mex. Fís.* **51** (2005) 53.
12. N. Atenco-Analco, F. Pérez-Rodríguez, and N. M. Makarov, *Appl. Surf. Sci.* **212-213** (2003) 782. N.
13. N. Atenco-Analco, N.M. Makarov, F. Pérez-Rodríguez, *Superficies y Vacío* **16** (2003) 7.
14. G. H. Cocoletzi, W. L. Mochán, *Phys. Rev. B* **39** (1989) 8403.
15. G. H. Cocoletzi, A. Ramírez-Perucho, W. L. Mochán, *Phys. Rev. B* **44** (1991) 11514.
16. S. Nojima, *Phys. Rev. B* **57** (1998) R2057.
17. S. Nojima, *Phys. Rev. B* **59** (1999) 5662.
18. E.L. Ivchenko, A.N. Poddubnyĭ, *Phys. Solid State* **48** (2006) 581.
19. B. Flores-Desirena, A. Silva-Castillo, and F. Pérez-Rodríguez, *J. Appl. Phys.* **93** (2003) 3308.
20. A. Silva-Castillo and F. Pérez-Rodríguez, *J. Appl. Phys.* **90** (2001) 3662.
21. N. Atenco-Analco, F. Pérez-Rodríguez, and J. Madrigal-Melchor, *Rev. Mex. Fís.* **48** (2002) 197.
22. P. Halevi, in Spatial Dispersion in *Solids and Plasmas, edited by P. Halevi, Electromagnetic Waves-Recent Developments in Research*, **1** (Elsevier, Amsterdam, 1992), Chap. 6.
23. L. C. Andreani, R. C. Iotti, R. Schwabe, F. Pietag, V. Gottschalch, A. Bitz, and J. L. Staehli, *Physica E* **2** (1998) 151.
24. V.A. Kosobukin, *Phys. Stat. Sol. (b)* **208** (1998) 271.
25. Z.K. Tang, A. Yanase, T. Yasui, Y. Segawa, and K. Cho, *Phys. Rev. B* **71** (1993) 1431.
26. Z.K. Tang, A. Yanase, Y. Segawa, N. Matsuura, and K. Cho, *Phys. Rev. B* **50**, (1995) 2640.
27. H. Suzuura, T. Tsujikawa, and T. Tokihiro, *Phys. Rev. B* **53** (1996) 1294.
28. T. Mita and N. Nagasawa, *Solid State Commun.* **44** (1982) 1003.
29. A. V. Kavokin, G. Malpuech, and G. Panzarini, *Phys. Stat. Sol. (b)* **216** (1999) 31.
30. F. G. Bass, I. M. Fuks, *Wave Scattering from Statistically Rough Surfaces* (Pergamon Press, New York, 1979).
31. A. R. McGurn, A. A. Maradudin, *Phys. Rev. B* **30** (1984) 3136.
32. N. Atenco-Analco, Ph. D. Thesis (BUAP, Puebla, 2004).
33. L.C. Andreani, G. Panzarini, A.V. Kovokin, M.R. Vladimirova, *Phys. Rev. B* **57** (1998) 4670.